Current Biology *16*, 1183–1193, June 20, 2006 DOI 10.1016/j.cub.2006.05.050

Article

Weckle Is a Zinc Finger Adaptor of the Toll Pathway in Dorsoventral Patterning of the *Drosophila* Embryo

Li-Ying Chen,[1,4] Juinn-Chin Wang,[1,4] Yann Hyvert,[2] Hui-Ping Lin,[1] Norbert Perrimon,[3] Jean-Luc Imler,[2] and Jui-Chou Hsu[1,*]

[1] Institute of Molecular Medicine
Department of Life Science
National Tsing Hua University
Hsinchu
Taiwan 30034
Republic of China

[2] Institut de Biologie Moléculaire et Cellulaire
UPR 9022 du CNRS
15 rue René Descartes
67084 Strasbourg Cedex
France

[3] Department of Genetics
Howard Hughes Medical Institute
Harvard Medical School
Boston, Massachusetts 02215

Summary

Background: The *Drosophila* Toll pathway takes part in both establishment of the embryonic dorsoventral axis and induction of the innate immune response in adults. Upon activation by the cytokine Spätzle, Toll interacts with the adaptor proteins DmMyD88 and Tube and the kinase Pelle and triggers degradation of the inhibitor Cactus, thus allowing the nuclear translocation of the transcription factor Dorsal/Dif. *weckle* (*wek*) was previously identified as a new dorsal group gene that encodes a putative zinc finger transcription factor. However, its role in the Toll pathway was unknown.

Results: Here, we isolated new wek alleles and demonstrated that *cactus* is epistatic to *wek*, which in turn is epistatic to *Toll*. Consistent with this, Wek localizes to the plasma membrane of embryos, independently of Toll signaling. Wek homodimerizes and associates with Toll. Moreover, Wek binds to and localizes DmMyD88 to the plasma membrane. Thus, Wek acts as an adaptor to assemble/stabilize a Toll/Wek/DmMyD88/Tube complex. Remarkably, unlike the *DmMyD88/tube/pelle/cactus* gene cassette of the Toll pathway, *wek* plays a minimal role, if any, in the immune defense against Gram-positive bacteria and fungi.

Conclusions: We conclude that Wek is an adaptor to link Toll and DmMyD88 and is required for efficient recruitment of DmMyD88 to Toll. Unexpectedly, *wek* is dispensable for innate immune response, thus revealing differences in the Toll-mediated activation of Dorsal in the embryo and Dif in the fat body of adult flies.

*Correspondence: lshsu@life.nthu.edu.tw
[4] These authors contributed equally to this work.

Introduction

The *Drosophila* Toll initiates an apparently linear signal transduction pathway to regulate the establishment of embryonic dorsoventral polarity [1–3]. Toll transmembrane receptor is uniformly expressed along the circumference of embryo but is ventrally activated by its ligand Spätzle. Spätzle is synthesized as an inactive precursor that is processed to its active form on the ventral side of the embryo by the serine protease Easter [4, 5]. Easter is the last component of a proteolytic cascade that also involves the products of the genes *gastrulation defective* and *snake*. The processed dimeric Spätzle interacts with two Toll ectodomains and initiates signaling [6, 7]. The intracellular domain of Toll contains a homotypic Toll/IL-1R (TIR) domain. After activation, Toll, via two adaptor proteins DmMyD88 and Tube, activates a death domain-containing kinase, Pelle, that in turn triggers degradation of the IκB-like inhibitor, Cactus, and the subsequent nuclear translocation of Dorsal (a member of the NF-κB family of transcription factors) [8–14]. The zygotic genes *twist* and *snail* are activated by peak levels of Dorsal on the ventral side of the embryos, while *zerknullt* (*zen*) and *decapentaplegic* (*dpp*) are derepressed by the absence of Dorsal on the dorsal regions [15].

DmMyD88 contains a N-terminal death domain, followed by a TIR domain and a C-terminal tail [9, 10, 16], while Tube possesses a bivalent death domain [8]. Prior to Toll activation, DmMyD88 and Tube, via death domain interactions, form a presignaling complex [8]. However, DmMyD88 is not detectably bound to nonactivated Toll, even though DmMyD88/Tube is membrane localized [8, 17]. It was postulated that DmMyD88 associates with Toll directly via weak interaction or indirectly through other molecules at plasma membrane [8]. Upon Toll activation, Pelle binds to the DmMyD88/Tube complex. Here, we demonstrate that *weckle* (*wek*), a recently identified new locus controlling dorsoventral patterning of the embryo [18], encodes an adaptor protein that links both Toll and DmMyD88 and is required for the membrane localization of DmMyD88.

The Toll pathway is also involved in the innate immune response in adult flies and mediates the response against most Gram-positive bacteria and fungi, while the Imd pathway mediates the immune response against Gram-negative bacteria [19]. Upon immune challenge, Spätzle is proteolytically cleaved to an active form by the serine protease Spätzle-processing enzyme (SPE), which participates in proteolytic cascades different from that operating in the embryo [20]. Active Toll on fat body cells transmits signal through DmMyD88/Tube/Pelle/Cactus to the cytoplasmic Dorsal-related immunity factor (Dif). The translocation of Dif into the nucleus activates the transcription of the genes encoding the antifungal peptides Drosomycin and Metchnikowin [21, 22]. Thus, although the upstream activating serine proteases and the most downstream NF-κB-like transcription factors (Dorsal versus Dif) differ, the

Spätzle-Toll-Cactus signaling cassette is well conserved in both the embryonic dorsoventral patterning and later in the humoral immune defense mediated by the fat body in adults. The *Drosophila* genome encodes a total of nine Toll receptors [23]. Apart from Toll, two other members of the family, Toll-5 and Toll-9, can signal to activate the *drosomycin* gene promoter [23, 24]. However, these receptors cannot substitute for Toll, and *drosomycin* induction is strongly decreased in *Toll*-deficient flies [25]. The other members of the family (18w/Toll-2; Toll-3, Toll-4, Toll-6, Toll-7, and Toll-8/Tollo) do not activate the *drosomycin* promoter [23, 24, 26]. The function of Toll-like receptors therefore remains mysterious.

Luschnig et al. identified *wek* as a new maternal gene involved in dorsoventral axis determination [18]. *wek* is allelic to *l(2)35Ea*, which was annotated to encode a zinc finger transcription factor [18, 27]. However, the role of *wek* in the Toll pathway has not been characterized. Here, we report the isolation of new alleles of *wek* and establish that *wek* is epistatic to *Toll*. Interestingly, Wek homodimerizes and localizes to the plasma membrane of the syncytial embryo, instead of the nucleus. Consistent with this, we found that Wek associates with both Toll and DmMyD88 and is required for the membrane localization of DmMyD88. Hence, Wek functions as an adaptor to link Toll and DmMyD88. Unexpectedly, we observed that *wek* is dispensable for the innate immune response, thus revealing differences in the Toll-mediated activation of Dorsal in the embryo and Dif in the fat body of adult flies.

Results

wek Mutations Generate Dorsalized Phenotypes

lotus root (*lor*, named after its strongly dorsalized cuticular structures resembling the morphology of lotus root) was isolated from a large genetic screen for EMS-induced, zygotic lethal mutations with maternal effects (N.P., C. Arnold, and A. Lanjuin, unpublished data). Embryos derived from mothers homozygous mutant for *lor* in the germline (referred to as *lor* GLC embryos) develop dorsalized cuticular structures with a range of phenotypes (Table 1): 33% of *lor* GLC embryos show moderately dorsalized phenotype (D1 [28]) with the dorsolaterally derived filzkörper but lacking the eight ventrally derived denticle belts (Figure 1C). Fifty-nine percent of embryos show weak dorsalized phenotypes (D2–3), as they still contain both filzkörper and a few denticle belts (Figure 1D). Surprisingly, 8% of embryos hatched. Even the embryos laid by a single female showed these variable dorsalized phenotypes. The severity of the

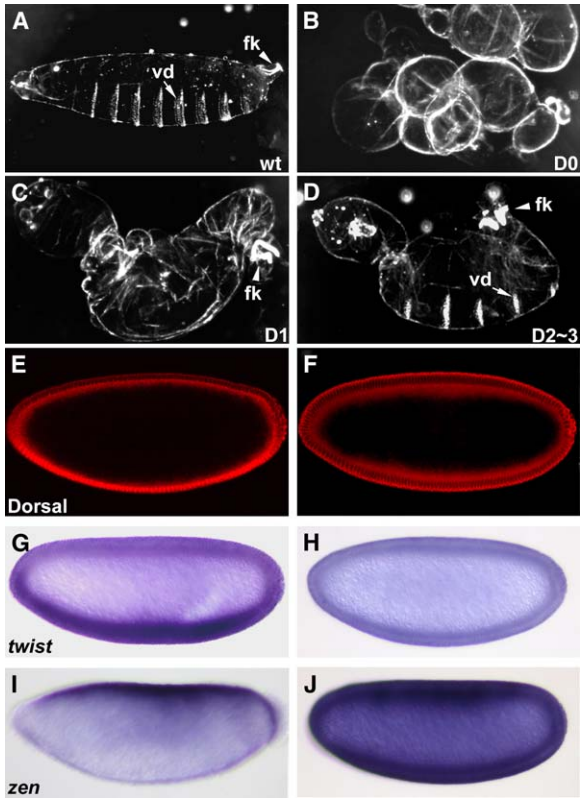

Figure 1. *wek* Is Required for Dorsoventral Patterning of *Drosophila* Embryos

All embryos (except that in [B]) are oriented with the anterior end to the left and the dorsal side up. (A, E, G, and I) Wild-type embryos. (B) Embryos laid by wek^{RAR14} GLC females. (C and D) Embryos laid by wek^{lor} GLC females. (F, H, and J) Embryos laid by wek^{EX14} GLC females. (A–D) Cuticle preparations. The arrow points to the denticle belts and the arrowhead to the filzkörper. Phenotypes in (B), (C), and (D) correspond to D0, D1, and D2–3 class, respectively. (E and F) Wild-type and wek^{EX14} GLC embryos stained with anti-Dorsal antibody. In situ hybridization of *twist* (G and H) and *zen* (I and J) in wild-type and wek^{EX14} GLC embryos.

Table 1. Mutant Phenotypes of *wek*

Phenotypes/ alleles	wek^{lor} (n = 90)	wek^{RAR14} (n = 96)	wek^{EX14} (n = 85)	wek^{EX14}; Tl^{r4}/+ (n = 107)	wek^{EX14}; Pll^{7}/+ (n = 97)	wek^{EX14}; Tub^{2}/+ (n = 76)	Wek^{lor}/wek^{EX14} (n = 27)	Wek^{lor}/wek^{EX14}; Tl^{9Q}/+ (n = 76)	Tl^{9Q}/+ (n = 21)
D0	0	12%	51%	97%	92%	96%	0	0	0
D1	33%	81%	49%	3%	8%	4%	56%	76%	0
D2–3	59%	7%	0	0	0	0	44%	0	0
wt	8%	0	0	0	0	0	0	0	0
L	0	0	0	0	0	0	0	24%	0
V	0	0	0	0	0	0	0	0	100%

The classification of phenotypes is according to Anderson et al. [28]. Dorsalized embryos (D) are characterized by the loss of ventral structures and an expansion of more dorsally derived structures. D0 embryos lack all lateral and ventral pattern elements, and D1 embryos lack ventral and lateral structures but retain dorsolaterally derived filzkörper. D2–3 cuticles contain both filzkörper and few ventral denticle belts, which may be reduced in width. Lateralized embryos (L) are more elongated and thinner than ventralized embryos and contain rings of laterally derived ventral denticle belts, which are finer than those produced by more ventral cells. Ventralized embryos (V) have belts of ventral denticles encircling the embryos, and all dorsal and lateral structures are eliminated.

dorsalized phenotypes observed is temperature insensitive (from 18ºC to 29ºC) and cannot be rescued zygotically by a paternal wild-type chromosome (data not shown). Therefore, *lor* represents a strictly maternal effect mutation.

lor is pupal lethal and failed to complement three alleles of *wek* [18, 27]: wek^{RAR14}, wek^{AM11}, and $wek^{l(2)05271}$, a P element insertion in the 5′ untranslated region (UTR) (at nucleotide 6) of *CG4148* (Figure S1A in the Supplemental Data available with this article online). Moreover, wek^{RAR14} GLC embryos develop stronger dorsalized phenotype than *lor*, with 12% of embryos secreting a hollow tube of dorsal epidermis (D0 phenotype) [28] (Figure 1B), while the remaining 81% and 7% of embryos were classified as D1 and D2–3 phenotype, respectively (Table 1). Thus, *lor* is allelic to *wek*, and we refer to it as such below. By performing imprecise excision of *l(2)05271*, we isolated wek^{EX14}, a putative RNA null allele (see below). wek^{EX14} GLC embryos exhibit the strongest dorsalized phenotype among the different *wek* alleles we characterized, with 51% and 49% embryos showing D0 and D1 phenotype, respectively (Table 1). One feature of this gene is that all the *wek* alleles characterized cause a wide range of dorsalized to wild-type phenotypes. This variability of phenotypes can also be detected in several *tube* alleles [29] and is very different from most alleles of other dorsal group genes, for which we observed a specific dorsalized phenotype. Remarkably, upon removal of one copy of *Toll*, *pelle*, or *tube*, the variable dorsalized phenotypes of wek^{EX14} GLC embryos were dramatically shifted to D0 phenotype (up to 97%; Table 1), revealing strong genetic interactions between these components.

The dorsalized phenotype of wek^{EX14} was further demonstrated by the lack of nuclear translocalization of Dorsal on the ventral side of wek^{EX14} GLC embryos (Figure 1F). In agreement with this observation, we did not observe the expression of Dorsal target gene *twist* in the ventral-most cells (Figure 1H). In contrast, *zen*, normally repressed by *dorsal*, is expanded to the ventral side (Figure 1J).

Characterization of the *wek* Gene

To characterize *wek* molecularly, we recovered the DNA region flanking $wek^{l(2)05271}$ by plasmid rescue and inverse PCR. Sequence analysis revealed that *l(2)05271* is inserted in the 5′ control region of the gene *CG4148* that encodes a C2H2 zinc finger-containing protein of 470 amino acids (Figure S1B). Our results were later confirmed by the online database of the *Drosophila* genome (http://flybase.org/). Ubiquitous expression of *tubulin* α*-CG4148* can completely rescue the dorsalized phenotype associated with wek^{EX14}, confirming that *wek* is *CG4148* (data not shown). Through a BLAST search, we identified three zinc finger-containing genes, *CG17568*, *CG10366*, and *CG6254*, as *wek* paralogs in the *Drosophila* genome. In addition to having high homology in the C-terminal zinc finger motifs, Wek also shows homology of 58%–65% and identity of 30%–43% in the N terminus with these three genes (Figure S1C). We refer to this region as the WekN domain (amino acids 1–103) and the C-terminal region as the WekC domain (amino acids 273–470) that contains the six zinc fingers. The rest of Wek was designated as WekM domain (amino acids 104–272) (Figure S1A). Although WekC shows high homology with several zinc finger proteins in mammals, we failed to identify a clear *wek* ortholog in mammals using WekN and WekM.

To identify the molecular lesions associated with *wek* mutants, we carried out genomic PCR from homozygous mutant larvae. wek^{RAR14} contains a premature stop codon at amino acid 88 and still possesses most of WekN, while wek^{lor} has two missense codons at amino acids 115 and 323 (Figure S1A). wek^{EX14} still carries a 1.1 kb fragment of the 3′ end of the P element, inserted (with reversed orientation) at nucleotide 13 of the 5′ UTR of *CG4148*, followed by a duplication of nucleotide 6–13. By performing reverse transcriptase-mediated PCR (RT-PCR) experiments, we observed that the mRNA level of *CG4148*, but not adjacent *Ku80*, was specifically abolished in homozygous wek^{EX14} larvae (Figure S1D), indicating that wek^{EX14} is a RNA null allele. This is consistent with our finding that wek^{EX14} GLC embryos exhibited the strongest phenotype.

Wek Localizes to Plasma Membrane

Zinc fingers are frequently encountered in transcription factors. To analyze the subcellular localization of Wek, we stained embryos of da-Gal4-driven *UAS-HA-wek* with HA antibody. We unexpectedly observed that Wek colocalizes with phosphotyrosine to the plasma membrane in syncytial wild-type embryos (Figures 2A–2A″). The membrane localization of endogenous Wek was confirmed using immunostaining with an antibody against the C-terminal Wek peptide (data not shown). To determine the region in Wek required for membrane localization, we generated HA-tagged deletion mutants of *wek* (Figure 2B). When expressed in embryos, all three constructs (WekN, WekNM, and WekC) localize to the plasma membrane, indicating that at least WekN or WekC alone is sufficient for membrane targeting (Figure 2C and data not shown). Activation of Toll on the ventral side of embryos was shown to lead to localized recruitment of Pelle and Tube to the plasma membrane [17]. To determine whether Wek distributes asymmetrically in response to Toll activation, we examined Wek localization with HA antibody in *da-Gal4; UAS-HA-Wek* embryos and *da-Gal4; UAS-HA-Wek; P[*$Toll^{10b}$*-bcd]* embryos where Toll-mediated signaling is ectopically oriented along the anteroposterior axis [30]. No significant asymmetry in the distribution of Wek across the dorsoventral (Figure 2D) or anteroposterior axis (data not shown) was detected, indicating that the membrane localization of Wek is independent of Toll signaling.

wek Acts Upstream of *cactus* but Downstream of *Toll*

The membrane localization of Wek prompted us to examine the genetic positioning of *wek* in the Toll pathway. As shown above, the nuclear translocation of Dorsal is affected in wek^{EX14} GLC embryos (Figure 1F), indicating that *wek* acts upstream of *dorsal*. To analyze the relationship between *wek* and *cactus*, we examined the embryos produced by wek^{lor} $cactus^{A2}$ double-mutant females. wek^{lor} is a weak dorsalizing mutation (mainly D2; Table 1), and wek^{lor} embryos lack *twist* expression (data not shown). $cactus^{A2}$ embryos exhibit strong ventralized phenotype (Figure 3A), and the laterally derived cephalic fold initiates dorsally after the onset of

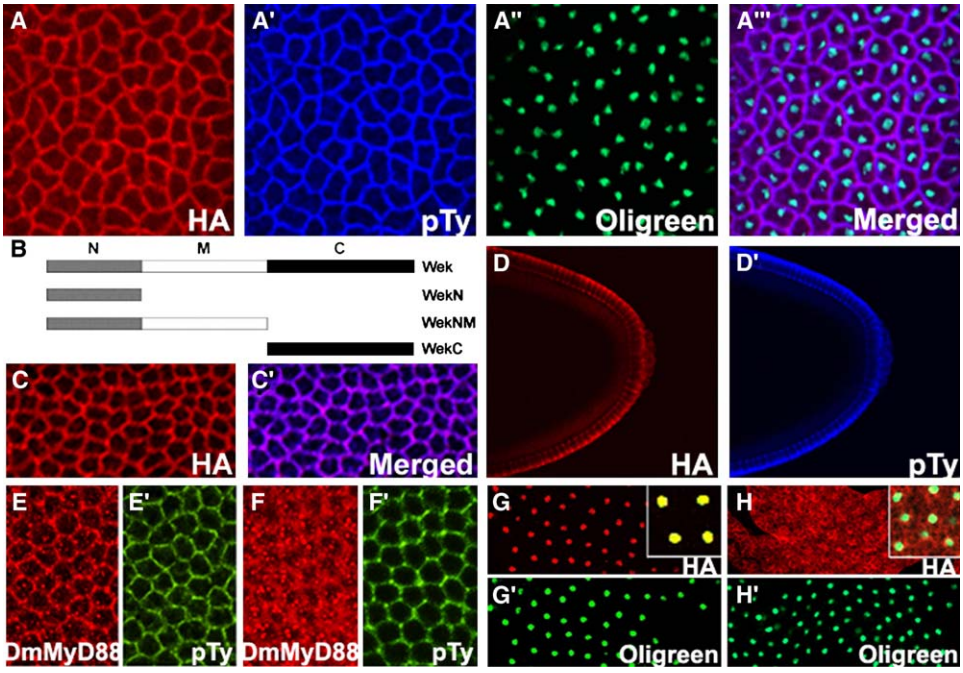

Figure 2. Distribution of Wek Derivatives in Early Embryogenesis and Fat Body

(A–A‴) Lateral surface views of syncytial embryos of *da-Gal4*-driven HA-Wek triple labeled with anti-HA (red), anti-phosphotyrosine (blue), and oligreen (green). HA-Wek colocalizes with phosphotyrosine to the plasma membrane. As a control, no HA signal was detected in the absence of *da-Gal4*.

(B) Diagram of UAS-driven transgenes of Wek derivatives.

(C and C′) Embryos of *da-Gal4*-driven HA-WekN double labeled with anti-HA (red) and anti-phosphotyrosine (blue).

(D and D′) Longitudinal cross-sections of embryos of *da-Gal4*-driven HA-Wek double labeled with anti-HA (red) and anti-phosphotyrosine (blue). There was no detectable asymmetry in the distribution of Wek across the dorsoventral axis. Embryos are oriented with the anterior end to the left and the dorsal side up.

(E and E′) Lateral surface views of wild-type embryos stained for DmMyD88 (red) and phosphotyrosine (green).

(F and F′) Lateral surface views of wek^{EX14} embryos stained for DmMyD88 (red) and phosphotyrosine (green). DmMyD88 became diffusive in the cytosol.

(G–H) Localization of *yolk-Gal4*-driven Wek derivative proteins (red) in the fat body of third instar larvae. Full-length Wek (G) localized to the nucleus (green), while WekN (H) localized to cytosol.

gastrulation (Figure 3C). Interestingly, wek^{lor} $cactus^{A2}$ double-mutant embryos exhibited a lateralized phenotype with rings of laterally derived ventral denticle belts, which are finer than those produced by more ventral cells (Figure 3B [31]). Consistent with this, we found that the cephalic folds are prominent at both dorsal and ventral positions (Figure 3D). Moreover, *zen* expression is absent on the dorsal side of these embryos (Figure 3G, compare with Figures 3E and 3F), but in contrast, moderate levels of Dorsal were detected in this region (Figure 3H). Together, our results indicate the loss of dorsal-most pattern elements exerted by the expansion of lateral structure (L1 with polarity) [31]. Previously, Roth et al. [31] showed that double mutants of $cactus^{A2}$ and weakly dorsalizing mutants of $spätzle^{67}/spätzle^{m7}$ (D2) also result in lateralized embryos (L1 with polarity). Thus, we conclude that *cactus* is epistatic to *wek*.

To order Wek in the pathway with respect to Toll, we generated wek^{lor}/wek^{EX14}; $Toll^{9Q}$/+ double mutants. $Toll^{9Q}$ encodes a constitutively active Toll receptor, and $Toll^{9Q}$/+ females produce ventralized embryos (Figure 3I). Although *wek* is pupal lethal, some wek^{lor}/wek^{EX14} transheterozygotes survived but with crooked legs [27]. Embryos laid by such females exhibited variable dorsalized phenotypes (56% and 44% of D1 and D2–3, respectively) that were weaker than those of wek^{EX14} but stronger than those of wek^{lor} GLC embryos (Table 1). Interestingly, embryos produced by wek^{lor}/wek^{EX14}; $Toll^{9Q}$/+ females exhibited biphasic phenotypic distribution, with 76% and 24% having moderately dorsalized (D1) and lateralized phenotypes, respectively. No weak dorsalized phenotypes (D2–3) were detected (Figures 3J and 3K). Previously, Hecht and Anderson [29] showed that double mutants of $Toll^{9Q}$ with moderately dorsaling (D1) *pelle* or *tube* alleles result in moderately dorsalized embryos (D1); however, weakly dorsalizing (D2–3) *pelle* or *tube* alleles with $Toll^{9Q}$ result in lateralized embryos. Since wek^{lor}/wek^{EX14} embryos exhibit both D1 as well as D2–3 dorsalized phenotypes, the simultaneous detection of D1 and lateralized phenotypes (but the absence of D2) in *wek; Toll* double-mutant embryos may simply reflect the sum of phenotypes of moderately dorsaling (D1) and weakly dorsalizing *wek* (D2–3) with $Toll^{9Q}$. Thus, like *tube* and *pelle*, *wek* is epistatic to *Toll* in the generation of the dorsoventral pattern.

Wek Forms Dimers and Specifically Associates with Toll and DmMyD88

The observation that Wek localizes to the cell surface and *wek* acts downstream of *Toll* prompted us to

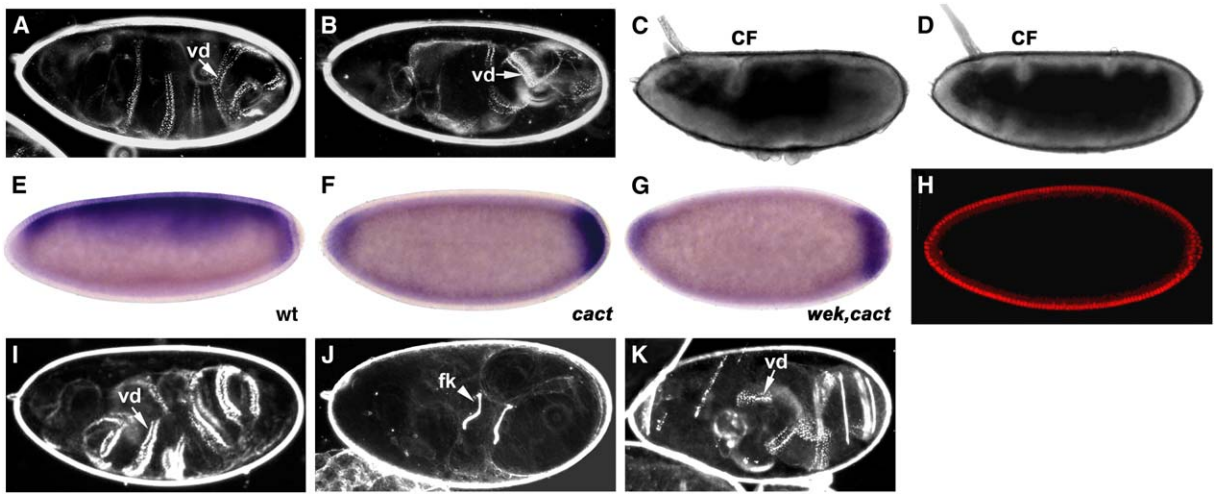

Figure 3. *cactus* Is Epistatic to *wek*, which in Turn Is Epistatic to *Toll*

Cuticle preparation of $cactus^{A2}$ GLC embryos (A) and wek^{lor} $cactus^{A2}$ double-mutant GLC embryos (B). *cactus* embryos show strongly ventralized phenotype, but wek^{lor} $cactus^{A2}$ double-mutant embryos show lateralized phenotype, as revealed by the presence of rings of laterally derived ventral denticle belts. Gastrulation patterns of $cactus^{A2}$ GLC embryos (C) and wek^{lor} $cactus^{A2}$ double-mutant GLC embryos (D). Anterior is to the left, and dorsal is up. CF, cephalic fold. In situ hybridization of *zen* in wild-type (E), $cactus^{A2}$ (F), and wek^{lor} $cactus^{A2}$ double-mutant embryos (G). Anterior is to the left, and dorsal is up. *zen* is expressed only at the poles of ventralized and lateralized embryos. (H) wek^{lor} $cactus^{A2}$ double-mutant GLC embryos stained with anti-Dorsal antibody. Cuticle preparation of embryos laid by $Toll^{9Q}$/+ heterozygous mothers (I) and by wek^{lor}/wek^{EX14}; $Toll^{9Q}$/+ mothers (J and K). $Toll^{9Q}$ causes a strongly ventralized cuticle. Seventy-six percent of embryos derived from wek^{lor}/wek^{EX14}; $Toll^{9Q}$/+ mothers show a moderately dorsalized phenotype (J), and 24% of embryos show a lateralized phenotype (K). The arrow points to the denticle belts and the arrowhead to the filzkörper.

investigate the molecular role of Wek in the Toll pathway. By performing yeast two-hybrid tests, we detected a weak interaction between full-length Wek, indicating that Wek might form homodimers (Figure 4A). To define specific domains in Wek that are responsible for the dimerization, we carried out deletion mapping studies. Although zinc finger motifs can mediate protein-protein interactions [32], we found that WekN, but not WekM and WekC, strongly interacts with full-length Wek and WekNM in pairwise experiments (Figure 4A), raising the possibility that the direct interaction between Wek is mediated through WekN. Since WekN alone, when fused with the Gal4 DNA binding domain, causes autoactivation in a two-hybrid assay (data not shown), we demonstrated the direct binding between WekN in transfected S2 cells with epitope-tagged constructs. As expected, WekN coimmunoprecipitated with itself and full-length Wek, but not WekM and WekC (Figure 4B). Thus, WekN is a dimerization domain. Interestingly, wek^{RAR14} allele encodes a truncated protein with most of the WekN domain and still retains partial activity, demonstrating the importance of WekN to mediate Toll activation.

Upon Toll homodimerization, the preexisting DmMyD88/Tube complexes will be recruited to the cell membrane, where it binds and activates Pelle kinase that leads to the degradation of Cactus [8]. We further investigated whether Wek interacts with the components of Toll/DmMyD88/Tube/Pelle complex in transfected S2 cells. Remarkably, we detected interactions between Wek and the intracellular domain of Toll. Similar interactions were detected with a constitutively active version of the receptor ($Toll^{\Delta LRR}$ [10]) and a nonactivated version (TollΔN4 [7]) (Figure 4C). A positive interaction was also observed with Toll-9 and to a lesser extent Toll-5, but not with Toll-6, Toll-7, and Toll-8, indicating that the interaction of Wek with TIR domains is very specific (Figure 4C for Toll, Toll-8, and Toll-9 and data not shown for Toll-5, Toll-6, Toll-7). Interestingly, Wek also associates with DmMyD88, but not Pelle, Dorsal, and Dif (Figure 4C and data not shown). Moreover, Wek does not interact with Tube in yeast two-hybrid assays. Hence, Wek functions as an adaptor protein to mediate the assembly of Toll/Wek/DmMyD88 complexes. It was shown that, before Toll activation, DmMyD88 is membrane associated but fails to bind Toll [8]. To determine whether Wek is the missing link that bridges Toll and DmMyD88, we examined the localization of DmMyD88 in the absence of Wek. Interestingly, the distribution of DmMyD88 in wek^{EX14} GLC embryos became diffusive in the cytosol (compare Figures 2E and 2F), and this change in localization was observed across the dorsoventral axis (data not shown), indicating that Wek plays an important role to localize DmMyD88 to the cell surface no matter the activation status of Toll.

To further identify the domains in Wek required for interaction with Toll and DmMyD88, we cotransfected either *Toll* or *DmMyD88* into S2 cells with different truncated versions of *wek*. Interestingly, all three individual domains of Wek form stable complexes with Toll (Figure 4D), a result consistent with the observation that WekN and WekC alone are sufficient for membrane targeting. In contrast, WekM and WekC, but not the dimerizing WekN domain, interact with DmMyD88 (Figure 4E). We then examined whether DmMyD88-mediated association with Wek is achieved through its death domain, its TIR domain or the C-terminal unique region [10]. Wek weakly interacted with the isolated

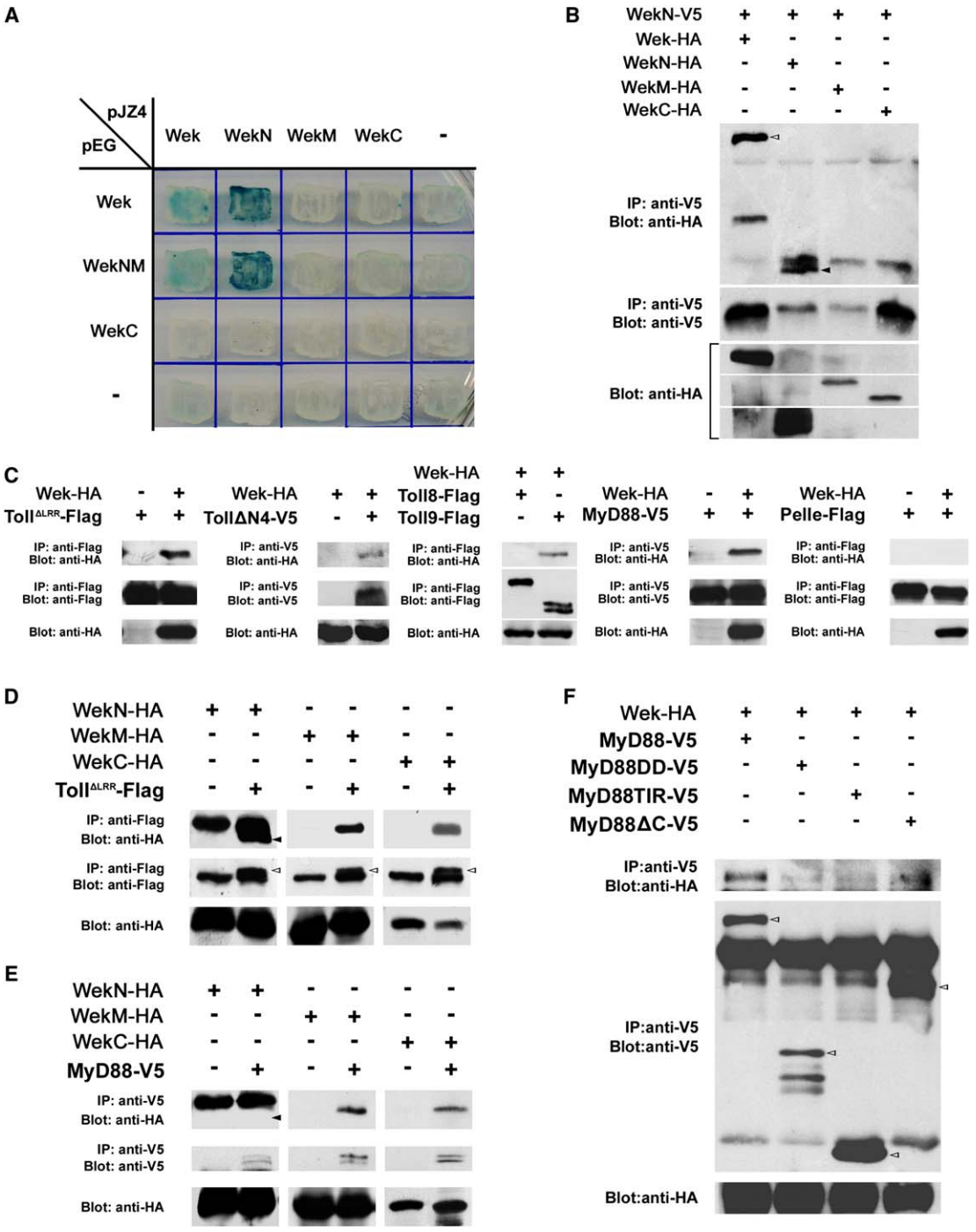

Figure 4. Molecular Interaction among Wek, Toll, DmMyD88, and Pelle and the Domains Involved

(A and B) Wek forms dimers via WekN domain. (A) The yeast two-hybrid assay shows that full-length Wek can self-associate and interacts specifically with WekNM. In addition, WekN strongly interacts with both full-length Wek and WekNM. (B) WekN coimmunoprecipitates with full-length Wek and WekN, but not WekM and WekC, in transfected S2 cells. Cells were cotransfected with V5-tagged WekN and different HA-tagged Wek derivatives. Immunoprecipitation was performed with anti-V5 and analyzed by immunoblotting with anti-HA. Open arrowhead: expected size of full-length Wek. Arrowhead: expected size of WekN.

(C) Wek selectively associates with Toll, Toll-9, and DmMyD88 but not Pelle. S2 cells were cotransfected with HA-tagged Wek and either Flag-tagged Toll$^{\Delta LRR}$, Flag-tagged TollΔN4, Flag-tagged Toll-8, Flag-tagged Toll-9, V5-tagged MyD88, or Flag-tagged Pelle.

(D and E) Domains required in Wek to interact with either Toll or MyD88. Flag-tagged Toll$^{\Delta LRR}$ (D) or V5-tagged DmMyD88 (E) was cotransfected with different HA-tagged Wek derivatives. Each individual domain of Wek is sufficient to associate with the intracellular domain of Toll. However, WekM and WekC, but not WekN, associates with MyD88. Arrowheads: expected size of WekN. Open arrowheads: expected size of Toll$^{\Delta LRR}$. The additional intense bands in (D) correspond to the light chains and heavy chains of anti-Flag antibodies, respectively.

(F) Domain required in MyD88 to interact with Wek. S2 cells were cotransfected with HA-tagged Wek and different V5-tagged MyD88 derivatives. Upon removal of any regions of MyD88, the interaction between Wek and MyD88 was greatly reduced. Open arrowheads: expected size of the corresponding DmMyD88 derivatives.

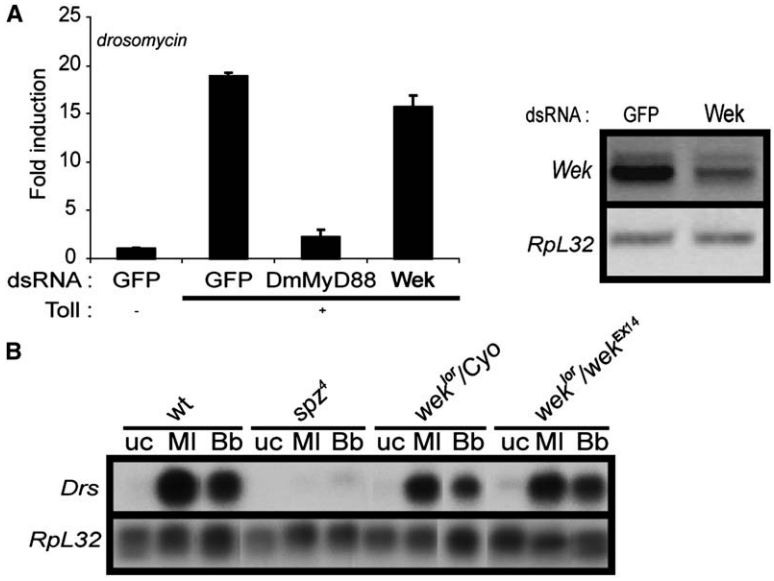

Figure 5. Wek Is Not Essential for the Induction of *drosomycin* Expression

(A) Knockdown of *wek* by RNAi does not affect induction of the *drosomycin* promoter activity by Toll in S2 cells. S2 cells were cotransfected with a metallothionein-Toll expression vector, the indicated double-stranded (ds) RNA, and a reporter construct expressing luciferase under the control of the *drosomycin* promoter. Cells were left untreated (−) or induced with $CuSO_4$ (+). The data represent the mean ± standard deviation of triplicates. The reduction of *wek* mRNA level in dsRNA-treated cells was verified by semiquantitative RT-PCR (right panel). mRNA for the ribosomal protein RpL32 was used as a control.

(B) Inducible expression of *drosomycin* is not reduced in transheterozygous *wek* mutant flies. Heterozygous and transheterozygous *wek* mutant flies were unchallenged (uc) or challenged with the Gram-positive bacteria *Micrococcus luteus* (Ml), or the entomopathogen fungus *Beauveria bassiana* (*Bb*) and analyzed by RNA blotting 24 hr later. Wild-type (w^-) and spz^4 (Toll pathway) flies were used as control. Quantification by phosphorimaging and normalization for the loading control *RpL32* indicate that *drosomycin* expression levels in heterozygote and transheterozygote flies represent, respectively, 76% and 70% of the expression in w^- flies for *M. luteus*, and 68% and 90% for *B. bassiana*.

TIR domain and death domain of DmMyD88 (Figure 4F), indicating that cooperative binding between different domains of DmMyD88 and Wek is required for the stable association. Interestingly, Wek also weakly interacted with a C-terminally truncated version of DmMyD88, indicating that the C-terminal extension, which is functionally important [33], participates in the interaction with Wek. Together, our results suggest that Wek is targeted to the plasma membrane through multiple contacts with Toll and DmMyD88.

wek and the Innate Immune Response

We next addressed the question of the role of *wek* in the Toll-mediated regulation of *drosomycin* expression. *wek* is expressed in immune-responsive, macrophage-like tissue culture S2 cells, as well as in the main tissue involved in the humoral immune response, the fat body (see below). Remarkably, in both larval and adult fat body, we found that HA-tagged Wek and WekNM preferentially accumulate in the nucleus (Figure 2G and data not shown), while WekN and WekC remain in the cytosol (Figure 2H and data not shown). This result, which was confirmed for the endogenous protein, suggests that Wek functions differently in the early embryo and in the fat body in adults.

We first attempted to trigger signaling by overexpressing *wek* in transfected S2 cells and failed to detect induction of a *drosomycin* reporter gene. Similar results were obtained in vivo, upon overexpression of *wek* in the fat body of females using the UAS-Gal4 system and a *yolk* driver (data not shown). RNAi experiments in S2 cells further showed that depletion of *wek* mRNA had minimal, if any, effect on induction of the *drosomycin* promoter by Toll. By contrast, knockdown of *DmMyD88* mRNA by RNAi dramatically reduced the activity of the *drosomycin* promoter (Figure 5A). In addition, overexpression of isolated domains from Wek (N, M, or C) in S2 cells did not interfere with Toll signaling, as would be expected for an adaptor molecule interacting with different components of a complex. By contrast, the TIR domain of DmMyD88, the death domain of Pelle, and the Tube repeats of Tube have all been shown to block Toll signaling when overexpressed in S2 cells (data not shown) [9, 10, 34]. Thus, *wek* does not appear to be required for Toll-mediated induction of *drosomycin* in these cells. We confirmed this finding in vivo, using wek^{Ior}/wek^{EX14} transheterozygotes. Flies were challenged with the Gram-positive bacteria *Micrococcus luteus*, or the fungus *Beauveria bassiana*, two strong inducers of the Toll pathway, and expression of *drosomycin* mRNA was monitored by Northern blot. As shown in Figure 5B, there was no difference in the induction of *drosomycin* mRNA between heterozygote and transheterozygote flies, confirming that *wek* does not appear to play an essential role in the humoral innate immune response. Normal induction of *drosomycin* expression was also observed in double-heterozygote flies for wek^{EX14} and strong alleles of *DmMyD88*, *pelle*, or *tube* (data not shown). This result is surprising, as up to now all genes comprised in the *spätzle* to *cactus* gene cassette have been shown to function both in dorsoventral patterning and immunity. In order to address the differences in the regulation of Toll targets in the embryo and in the adult fat body, we attempted to study the induction of the *twist* promoter by the Toll pathway in S2 cells. Surprisingly, we found that Toll was not able to activate a *twist* reporter gene [35] in these cells. Similarly, overexpression of DmMyD88 and Pelle, which both lead to strong induction of the *drosomycin* promoter, did not affect the activity of the *twist* promoter (Figure S2). Only overexpression of Dorsal or Dif led to strong induction of the *twist* reporter. These data confirm the existence of differences in the regulation of *twist* and *drosomycin*, although Toll is both necessary and sufficient to regulate these genes in different contexts in vivo.

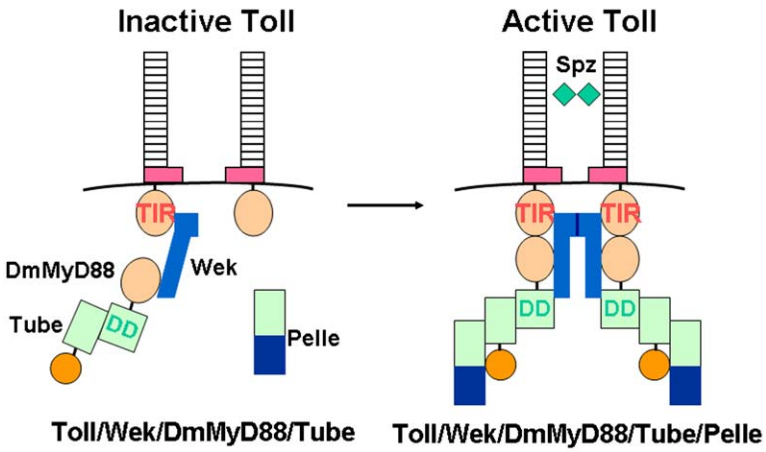

Figure 6. Model for Molecular Interactions between Components of the Toll Pathway

Prior to Toll activation, Wek interacts with Toll and recruits DmMyD88/Tube complex to form a relatively unstable Toll/Wek/DmMyD88/Tube presignaling complex on the membrane. The cysteine-containing motif (pink) of Toll self-inhibits Toll activation. Upon Toll dimerization by Spätzle, active Toll simultaneously recruits both DmMyD88 and Wek to form a more stable Toll/Wek/DmMyD88/Tube complex that activates Pelle. Wek can self-associate through the WekN domain.

Discussion

A New Component of the Toll Pathway

Signaling by Toll receptors, as well as by members of the IL-1R family, is mediated by the 150 amino acid TIR domain. TIR domains are believed to function as homotypic protein-protein interaction domains, like death domains. Interaction between the TIR domains of Toll and DmMyD88 is indeed suggested by coimmunoprecipitation experiments in cultured cells [8–10]. However, Moussian and collaborators failed to detect interaction between DmMyD88 and the Toll intracytoplasmic domain in yeast two-hybrid assays, although they readily detected interaction between DmMyD88 and Tube [16]. In addition, overexpression of the TIR domain of DmMyD88 leads to strong activation of the pathway, instead of behaving like a dominant negative, as one would expect for a domain-mediating interaction with upstream components of the pathway [9, 10]. Thus, there are indications that the situation may be more complex than initially assumed and involve a supplementary factor in the receptor complex. We now describe a zinc finger protein that functions as an adaptor in the Toll pathway. Our data clearly establish that efficient recruitment of DmMyD88 to Toll in the embryo requires Wek and that Wek is part of the Toll receptor complex. This model is supported by coimmunoprecipitations in *Drosophila* cultured cells, immunolocalization in embryos, and finally genetics, as embryos laid by *wek* mutant females exhibit similar phenotypes as other Toll pathway mutants. Furthermore, we demonstrated strong genetic interactions between *wek* and other genes of the Toll pathway. Interestingly, we noticed that Wek also interacts with Toll-9 and to a lesser extent Toll-5, but not with other members of the Toll family. Toll, Toll-9, and Toll-5 are the only members of the family that are able to activate the Toll pathway in tissue culture cells [23, 24], and hence there is a perfect correlation between the capacity to interact with Wek and the activation of the pathway.

Because DmMyD88 associates with active Toll [8], our observation that Wek is required to localize DmMyD88 to the cell surface even when Toll is active indicates that the physical interaction between active Toll and DmMyD88 alone might not be stable. This together with a series of binding results leads us to propose that, before Toll activation, Wek bridges Toll and the DmMyD88/Tube complex to assemble into a large Toll/Wek/DmMyD88/Tube presignaling complex on the membrane. Upon Toll activation, Toll can now simultaneously associate with both adaptors (DmMyD88 and Wek) to assemble a much more stable Toll/Wek/DmMyD88/Tube complex that leads to the differential association and activation of Pelle (Figure 6). This model not only explains why DmMyD88 is still membrane associated when Toll is inactive on the dorsal side of the embryo but also explains why Tube and DmMyD88 distribute asymmetrically along the dorsoventral axis with increased concentration along the ventral surface [8, 17]. In the absence of Wek, the weak association between active Toll and DmMyD88/Tube might either completely or partially abolish the recruitment and activation of Pelle to produce a range of dorsalized phenotypes. According to this model (Figure 6), active Toll interacts with a Spätzle dimer via its ectodomain and with a Wek dimer via its cytoplasmic tail. However, overexpression of Wek can not partially rescue the completely dorsalized phenotype of *spz* mutant embryos (J.-C.H., unpublished data), indicating that Wek alone is not sufficient to mediate Toll activation.

Although our genetic and biochemical data support that the zinc finger-containing Wek acts at the plasma membrane as an adaptor during dorsoventral patterning, Wek preferentially accumulates in the nucleus of fat body cells. Thus, we cannot completely exclude the possibility that Wek might have a nuclear function as well. This would be reminiscent of Armadillo, which acts not only as an adaptor of Cadherin but also as a transcription factor in the nucleus.

Wek and the Immune-Regulated Expression of *drosomycin*

Surprisingly, our data suggest that *wek* is not required for the Toll-mediated induction of the *drosomycin* gene in response to immune challenge. Indeed, we observed wild-type responses in the fat body of *wek* mutant flies, and in S2 cells depleted of *wek* mRNA by RNAi. This result might be explained by a different threshold level for *wek* function in development and immunity: the residual activity of the Toll pathway in

wek^{lor}/*wek*^{EX14} transheterozygote flies, and in *wek* dsRNA-treated S2 cells, could be sufficient for the immune response. We note, however, that experiments with DmMyD88 revealed on the contrary that the dorsoventral patterning function appears to be less sensitive than the immune function, as flies homozygote for the hypomorphic allele *DmMyD88*^{EP2133} are severely impaired in their host-defense functions [10], but not for dorsoventral patterning [33]. Thus, although we cannot formally rule out a role of *wek* in Toll-mediated immune defenses, the most likely explanation for our results is that induction of *drosomycin* expression by Toll in fat body and S2 cells does not depend on *wek*. This interpretation is supported by the fact that in the fat body Wek does not colocalize with Toll at the plasma membrane but rather preferentially localizes to the nucleus.

Differences between Toll signaling in the embryo and in adults have already been reported in several instances. The first difference pertains to the identity of the transcription factor induced, Dorsal in the embryo and Dif in adults [21, 22]. There is also convincing evidence that Toll not only signals to Cactus, but also induces phosphorylation of Dorsal [36]. In addition, differences were observed in the interaction of Dorsal and Dif with cofactors. For example, unlike Dorsal, Dif does not appear to interact and synergize with basic-helix-loop-helix transcription factors [37] or to be affected by the negative regulator WntD [38]. Conversely, the coactivator dTRAP80 modulates activation of Dif, but not Dorsal, in S2 cells [39]. Wek might therefore regulate a Dorsal-specific output of the Toll pathway. This hypothesis is, however, difficult to reconcile with the fact that Wek acts between two components of the pathway, Toll and DmMyD88, which are both required for activation of Dorsal in the embryo and Dif in adults. Furthermore, the proposed function of Wek as an adaptor that connects Toll and DmMyD88 does not explain why this factor is not required in adults and S2 cells. The most likely reason to explain this paradox is that another molecule substitutes for Wek in fat body and S2 cells. The three paralogs of *wek* (CG6254, CG17568, and CG10366) found in the *Drosophila* genome are prime candidates to carry this function and connect Toll to DmMyD88 in immune-competent cells. The first two contain both the N region and the zinc finger-containing C region, whereas the third one contains all three domains. However, RNAi-mediated silencing of these genes in S2 cells did not affect Toll signaling (data not shown). Thus, the identity of the factor that bridges Toll and DmMyD88 in fat body cells remains unknown at this stage.

The different requirement for Wek in embryos and adults may also reflect the presence of Dorsal and Dif in the Toll receptor complex. Because the NF-κB-like molecules targeted by Toll are different in the embryo and in adults, such a mechanism could provide an explanation for the embryo-specific phenotype of *wek* mutant flies. In support of this hypothesis, Cactus-bound Dorsal has been shown to form a complex with Tube and Pelle, in which Cactus may be phosphorylated by Pelle [40–42]. It is interesting to note that this hypothetic model of activation of Dorsal and Dif at the receptor complex is evocative of the activation of the transcription factor IRF7 by the kinase IRAK1 upon stimulation of TLR7 or TLR9 in mammalian cells [43].

Experimental Procedures

Drosophila Stocks and Genetic Crosses

Drosophila stocks were *wek*^{lor} and *wek*^{EX14} (this work), *yolk-Gal4* [10], and *cactus*^{A2} [31]. The *wek*^{RAR14}, *wek*$^{l(2)05271}$, *Toll*^{9Q}, *Toll*^{r4}, *pelle*^{7}, *tube*^{2}, and *da-Gal4* are described at Flybase and were obtained from the Bloomington Stock Center (Indiana). Unless specified, all the genetic crosses were performed at 25ºC.

Germline clones homozygous for *wek* and *wek*^{lor} *cactus*^{A2} double mutants were generated using the FLP-DFS technique [44]. *wek*^{EX14} was generated by mobilization of *wek*$^{l(2)05271}$ using Δ2-3 as a source of transposase. Individuals with *rosy*$^{-}$ were obtained, and then complementation tests, genomic PCR, and phenotypical analysis were carried out to verify the excision of *wek*$^{l(2)05271}$.

For the epistatic analysis between *wek* and *Toll*, we generated *wek*^{lor}/*wek*^{EX14}; *Toll*^{9Q}/+ females. Females of *wek*^{EX14}/Cyo were crossed to *wek*^{lor}/*Cyo; Toll*^{9Q}/+ males. From the progeny of this cross, we selected females of *wek*^{lor}/*wek*^{EX14}; *Toll*^{9Q}/+ and crossed them to wild-type males. *wek*^{lor}/*wek*^{EX14} adults have crooked legs. To unambiguously identify the presence of *Toll*^{9Q} in these females, individual females (with crooked legs) were sacrificed after they had laid eggs for 7 days, and then genomic PCR was performed to confirm the presence of G2970A nucleotide substitution of *Toll*^{9Q}. The primers used were 5′-AACCAGCATCGATGTGGATCA-3′ and 5′-AAGGCATCGAACTTCTTGTCC-3′. Embryos produced were examined in cuticle preparations.

Molecular Biology

Plasmids

pPAC-Toll$^{\Delta LRR}$ (pJL195), pPAC-MyD88 (pIL246), pPAC-pelle, pPAC-dorsal, and pPAC-dif are described [10]. For the expression of *wek* in S2 cells, the PCR fragments coding for amino acids 1–103, 104–272, 273–470, and 1–470 of Wek were cloned into pPAC to generate pPAC-WekN, pPAC-WekM, pPAC-WekC, and pPAC-Wek, respectively. PAc5.1/V5-TollΔN4 was made by subcloning the coding region of pUAST-TollΔN4 [7] into PAc5.1/V5 vector. For the expression of *wek* in transgenic flies, the PCR fragments coding for amino acids 1–103, 1–272, 273–470, and 1–470 of Wek were cloned into pPUAST vector to generate UAS-WekN, UAS-WekNM, UAS-WekC, and UAS-Wek, respectively. The tubulinα1-CG4148 was made by inserting PCR fragments coding for amino acids 1–470 of Wek into pCaSpeR-tubulinα1 vector [21]. For the expression of *wek* in yeast two-hybrid assays, the PCR fragments coding for amino acids 1–103, 1–261 (NM), 104–272, 273–470, and 1–470 of Wek were subcloned into pEG202 (with the LexA DNA binding domain) or pJZ4 (with the LexA activation domain). All the PCR fragments were checked by sequencing.

In Situ Hybridization, Antibody Staining, and Cuticle Preparation

For in situ hybridization, digoxigenin-labeled antisense RNA probes were synthesized from linearized *twist* and *zen* cDNA. Hybridization and histochemical detection using alkaline phosphatase were performed as described by Tautz and Pfeifle [45]. For immunostaining, embryos and fat body were fixed in 4% formaldehyde. The following primary antibodies were used: mouse anti-Dorsal (1:50; Hybridoma Bank), rabbit anti-MyD88 (1:1000 [8]), and rat anti-HA (1:250; Roche). Cy3- and Cy5-conjugated secondary IgGs are from Jackson ImmunoResearch Laboratories. Confocal microscopy was performed using a Zeiss Model Pascal. For cuticle preparation, embryos were collected 24 hr after laying, dechorionated in 50% bleach, devitellinized by vortex in equal volumes of heptane and methanol, and then mounted in a mixture of Hoyer's solution and lactic acid (2:1) [46].

Protein Interaction Assays

Yeast two-hybrid assays were performed according to the procedures described [47]. Various pEG202 and pJZ4 constructs were transformed into Y309 and RFY231 (with the LacZ reporter gene), respectively, followed by mating as described [48].

For S2 cell coimmunoprecipitation, S2 cells were grown at 25ºC in Schneider's medium (GIBCO/BRL) supplemented with 10% FCS. Cells (5 × 10^{6} cells per well) were transfected in 6-well dishes by Cellfectin Reagent (Invitrogen) with 1 μg each of expression vector. At 48 hr after transfection, S2 cells were collected, washed twice in PBS, and lysed for 1 hr at 4ºC in 150 μl of lysis buffer (20 mM

Tris [pH 7.5], 150 mM NaCl, 1% Triton X-100, and a protease inhibitor cocktail [Roche]), followed by centrifugation to pellet debris. Lysate (with 500 μg of total proteins) was incubated with primary antibodies (1 μg anti-FLAG [M2] [Sigma] and 1 μg anti-V5 [Invitrogen]) for 2 hr at 4ºC. Protein A Sepharose was then added and incubated 1 hr at 4ºC. Analysis was conducted using SDS-PAGE followed by Western blot using the ECL protocol (Amersham Pharmacia), anti-HA (1:1000), anti-Flag (1:1000), and anti-V5 (1:1000).

drosomycin Induction Assays

For ex vivo experiments, S2 cells were transfected in 6 cm diameter dishes by the calcium phosphate precipitation technique with 0.1 μg of a β-galactosidase expression vector, 0.1 μg of a *drosomycin*- or *twist*-luciferase reporter plasmid, and 1 μg of actin 5C- or metallothionein-driven expression vector [10, 23, 49]. For RNAi experiments, double-stranded (ds) RNA was produced as described [50]. Coding sequence DNA fragments (500–700 base pairs in length) from the genes to be inactivated were amplified by PCR using a 5′ T7 RNA polymerase binding site, purified, and subsequently used as templates for in vitro transcription using the Megascript T7 transcription kit (Ambion). Two dsRNAs corresponding to the 5′ end and 3′ end of *wek* were generated (using the primer pairs 5′-ACT GGGCAGCATGTTGTG-3′/5′-AGGACATAAAGGTTTCGTTG-3′ and 5′-AGCACGACATGCACGGCGG-3′/5′-ATGCAAAAAGGGCAGTTGT GTG-3′) and used with similar results. The dsRNA products were annealed by incubation at 65ºC for 30 min, followed by slow cooling to room temperature, and stored at −20ºC. dsRNA (4 μg) was used to cotransfect 6 cm diameter dishes of S2 cells with the reporter plasmid and metallothionein expression vectors. Forty-eight hours after transfection, cells were stimulated with 500 μM CuSO4 for 48 hr. Cells were then lysed in reporter lysis buffer, and luciferase activity was measured in a luminometer (BCL Book; Promega) immediately after addition of the substrate (luciferin; Promega). β-galactosidase was measured by using *o*-nitrophenyl-β-D-galactoside as a substrate, and the values were used to normalize for the variability in transfection efficiency.

For in vivo experiments, 2- to 4-day-old flies were pricked with a tungsten needle previously dipped into a concentrated culture of *Micrococcus luteus*. For fungal infection, anesthetized flies were shaken for 30 s on a Petri dish containing a sporulating culture of the entopathogen fungus *B. bassiana*. Following infections, flies were kept at 25ºC. Twenty-four hours later, RNA was extracted and analyzed by Northern blot. Quantification was done with a BAS2000Bio-Imager (Fujix), and data were standardized against the constitutively expressed RpL32 signal.

Supplemental Data

The Supplemental Data include Supplemental Experimental Procedures and two figures and can be found with this article online at http://www.current-biology.com/cgi/content/full/16/12/1183/DC1/.

Acknowledgments

We are grateful to J. Roote, Y. Engstrom, R.L. Finley, R. Steward, S.A. Wasserman, T. Ip, B. Moussian, C. Thummel, A. Bergmann, J. Grosshans, W.M. Gelbart, M. Levine, and DSHB for providing reagents and stocks, and to D. Ferrandon and S. Roth for critical reading of the manuscript and valuable suggestions. Grants from the National Science Council (94-2311-B-007-017) and the Technology Development Program of the Ministry of Economy, Taiwan, Republic of China to J.-C.H. and Ministère de la Recherche et de la Technologie (ACI Biologie du développement et physiologie integrative) to J.-L.I. are acknowledged. Y.H. is supported by a fellowship from the Ligue Nationale contre le Cancer.

Received: January 24, 2006
Revised: May 10, 2006
Accepted: May 17, 2006
Published: June 19, 2006

References

1. Stathopoulos, A., and Levine, M. (2002). Linear signaling in the Toll-Dorsal pathway of *Drosophila*: Activated Pelle kinase specifies all threshold outputs of gene expression while the bHLH protein Twist specifies a subset. Development *129*, 3411–3419.
2. Belvin, M.P., and Anderson, K.V. (1996). A conserved signaling pathway: The *Drosophila* Toll-Dorsal pathway. Annu. Rev. Cell Dev. Biol. *12*, 393–416.
3. Moussian, B., and Roth, S. (2005). Dorsoventral axis formation in the *Drosophila* embryo—Shaping and transducing a morphogen gradient. Curr. Biol. *15*, R887–R899.
4. Schneider, D.S., Jin, Y., Morisato, D., and Anderson, K.V. (1994). A processed form of the Spätzle protein defines dorsal-ventral polarity in the *Drosophila* embryo. Development *120*, 1243–1250.
5. DeLotto, Y., and DeLotto, R. (1998). Proteolytic processing of the *Drosophila* Spätzle protein by easter generates a dimeric NGF-like molecule with ventralising activity. Mech. Dev. *72*, 141–148.
6. Weber, A.N., Tauszig-Delamasure, S., Hoffmann, J.A., Lelièvre, E., Gascan, H., Ray, K.P., Morse, M.A., Imler, J.L., and Gay, N.J. (2003). Binding of the *Drosophila* cytokine Spätzle to Toll is direct and establishes signaling. Nat. Immunol. *4*, 794–800.
7. Hu, X., Yagi, Y., Tanji, T., Zhou, S., and Ip, Y.T. (2004). Multimerization and interaction of Toll and Spätzle in *Drosophila*. Proc. Natl. Acad. Sci. USA *101*, 9369–9374.
8. Sun, H., Towb, P., Chiem, D.N., Foster, B.A., and Wasserman, S.A. (2004). Regulated assembly of the Toll signaling complex drives *Drosophila* dorsoventral patterning. EMBO J. *23*, 100–110.
9. Horng, T., and Medzhitov, R. (2001). *Drosophila* MyD88 is an adapter in the Toll signaling pathway. Proc. Natl. Acad. Sci. USA *98*, 12654–12658.
10. Tauszig-Delamasure, S., Bilak, H., Capovilla, M., Hoffmann, J.A., and Imler, J.L. (2002). *Drosophila* MyD88 is required for the response to fungal and Gram-positive bacterial infections. Nat. Immunol. *3*, 91–97.
11. Shen, B., and Manley, J.L. (2002). Pelle kinase is activated by autophosphorylation during Toll signaling in *Drosophila*. Development *129*, 1925–1933.
12. Belvin, M.P., Jin, Y., and Anderson, K.V. (1995). Cactus protein degradation mediates *Drosophila* dorsal-ventral signaling. Genes Dev. *9*, 783–793.
13. Bergmann, A., Stein, D., Geisler, R., Hagenmaier, S., Schmid, B., Fernandez, N., Schnell, B., and Nüsslein-Volhard, C. (1996). A gradient of cytoplasmic Cactus degradation establishes the nuclear localization gradient of the *dorsal* morphogen in *Drosophila*. Mech. Dev. *60*, 109–123.
14. Roth, S., Stein, D., and Nüsslein-Volhard, C. (1989). A gradient of nuclear localization of the *dorsal* protein determines dorsoventral pattern in the *Drosophila* embryo. Cell *59*, 1189–1202.
15. Ray, R.P., Arora, K., Nüsslein-Volhard, C., and Gelbart, W.M. (1991). The control of cell fate along the dorsal-ventral axis of the *Drosophila* embryo. Development *113*, 35–54.
16. Charatsi, I., Luschnig, S., Bartoszewski, S., Nüsslein-Volhard, C., and Moussian, B. (2003). Krapfen/dMyd88 is required for the establishment of dorsoventral pattern in the *Drosophila* embryo. Mech. Dev. *120*, 219–226.
17. Towb, P., Galindo, R.L., and Wasserman, S.A. (1998). Recruitment of Tube and Pelle to signaling sites at the surface of the *Drosophila* embryo. Development *125*, 2443–2450.
18. Luschnig, S., Moussian, B., Krauss, J., Desjeux, I., Perkovic, J., and Nüsslein-Volhard, C. (2004). An F1 genetic screen for maternal-effect mutations affecting embryonic pattern formation in *Drosophila melanogaster*. Genetics *167*, 325–342.
19. Hoffmann, J.A. (2003). The immune response of *Drosophila*. Nature *426*, 33–38.
20. Jang, I.H., Chosa, N., Kim, S.H., Nam, H.J., Lemaitre, B., Ochiai, M., Kambris, Z., Brun, S., Hashimoto, C., Ashida, M., et al. (2006). A spätzle-processing enzyme required for Toll signaling activation in *Drosophila* innate immunity. Dev. Cell *10*, 45–55.

21. Meng, X., Khanuja, B.S., and Ip, Y.T. (1999). Toll receptor-mediated *Drosophila* immune response requires Dif, an NF-κB factor. Genes Dev. *13*, 792–797.
22. Rutschmann, S., Jung, A.C., Hetru, C., Reichhart, J.M., Hoffmann, J.A., and Ferrandon, D. (2000). The Rel protein DIF mediates the antifungal but not the antibacterial host defense in *Drosophila*. Immunity *12*, 569–580.
23. Tauszig, S., Jouanguy, E., Hoffmann, J.A., and Imler, J.L. (2000). Toll-related receptors and the control of antimicrobial peptide expression in *Drosophila*. Proc. Natl. Acad. Sci. USA *97*, 10520–10525.
24. Ooi, J.Y., Yagi, Y., Hu, X., and Ip, Y.T. (2002). The *Drosophila* Toll-9 activates a constitutive antimicrobial defense. EMBO Rep. *3*, 82–87.
25. Lemaitre, B., Nicolas, E., Michaut, L., Reichhart, J.M., and Hoffmann, J.A. (1996). The dorsoventral regulatory gene cassette spätzle/Toll/cactus controls the potent antifungal response in *Drosophila* adults. Cell *86*, 973–983.
26. Ligoxygakis, P., Bulet, P., and Reichhart, J.M. (2002). Critical evaluation of the role of the Toll-like receptor 18-Wheeler in the host defense of *Drosophila*. EMBO Rep. *3*, 666–673.
27. Ashburner, M., Misra, S., Roote, J., Lewis, S.E., Blazej, R., Davis, T., Doyle, C., Galle, R., George, R., Harris, N., et al. (1999). An exploration of the sequence of a 2.9-Mb region of the genome of *Drosophila melanogaster*: The *Adh* region. Genetics *153*, 179–219.
28. Anderson, K.V., Jürgens, G., and Nüsslein-Volhard, C. (1985). Establishment of dorsal-ventral polarity in the *Drosophila* embryo: Genetic studies on the role of the *Toll* gene product. Cell *42*, 779–789.
29. Hecht, P.M., and Anderson, K.V. (1993). Genetic characterization of *tube* and *pelle*, genes required for signaling between *Toll* and *dorsal* in the specification of the dorsal-ventral pattern of the *Drosophila* embryo. Genetics *135*, 405–417.
30. Huang, A.M., Rusch, J., and Levine, M. (1997). An anteroposterior Dorsal gradient in the *Drosophila* embryo. Genes Dev. *11*, 1963–1973.
31. Roth, S., Hiromi, Y., Godt, D., and Nüsslein-Volhard, C. (1991). *cactus*, a maternal gene required for proper formation of the dorsoventral morphogen gradient in *Drosophila* embryos. Development *112*, 371–388.
32. Liew, C.K., Simpson, R.J., Kwan, A.H., Crofts, L.A., Loughlin, F.E., Matthews, J.M., Crossley, M., and Mackay, J.P. (2005). Zinc fingers as protein recognition motifs: Structural basis for the GATA-1/friend of GATA interaction. Proc. Natl. Acad. Sci. USA *102*, 583–588.
33. Kambris, Z., Bilak, H., D'Alessandro, R., Belvin, M., Imler, J.L., and Capovilla, M. (2003). *DmMyD88* controls dorsoventral patterning of the *Drosophila* embryo. EMBO Rep. *4*, 64–69.
34. Norris, J.L., and Manley, J.L. (1995). Regulation of dorsal in cultured cells by Toll and tube: Tube function involves a novel mechanism. Genes Dev. *9*, 358–369.
35. Thisse, C., Perrin-Schmitt, F., Stoetzel, C., and Thisse, B. (1991). Sequence-specific transactivation of the *Drosophila twist* gene by the *dorsal* gene product. Cell *65*, 1191–1201.
36. Drier, E.A., Govind, S., and Steward, R. (2000). Cactus-independent regulation of Dorsal nuclear import by the ventral signal. Curr. Biol. *10*, 23–26.
37. Stein, D., Goltz, J.S., Jurcsak, J., and Stevens, L. (1998). The Dorsal-related immunity factor (Dif) can define the dorsal-ventral axis of polarity in the *Drosophila* embryo. Development *125*, 2159–2169.
38. Gordon, M.D., Dionne, M.S., Schneider, D.S., and Nusse, R. (2005). WntD is a feedback inhibitor of Dorsal/NF-κB in *Drosophila* development and immunity. Nature *437*, 746–749.
39. Park, J.M., Kim, J.M., Kim, L.K., Kim, S.N., Kim-Ha, J., Kim, J.H., and Kim, Y.J. (2003). Signal-induced transcriptional activation by Dif requires the dTRAP80 mediator module. Mol. Cell. Biol. *23*, 1358–1367.
40. Edwards, D.N., Towb, P., and Wasserman, S.A. (1997). An activity-dependent network of interactions links the Rel protein Dorsal with its cytoplasmic regulators. Development *124*, 3855–3864.
41. Yang, J., and Steward, R. (1997). A multimeric complex and the nuclear targeting of the *Drosophila* Rel protein Dorsal. Proc. Natl. Acad. Sci. USA *94*, 14524–14529.
42. Großhans, J., Bergmann, A., Haffter, P., and Nüslein-Volhard, C. (1994). Activation of the kinase Pelle by Tube in the dorsoventral signal transduction pathway of *Drosophila* embryo. Nature *372*, 563–566.
43. Moynagh, P.N. (2005). TLR signalling and activation of IRFs: Revisiting old friends from the NF-κB pathway. Trends Immunol. *26*, 469–476.
44. Chou, T.B., and Perrimon, N. (1996). The autosomal FLP-DFS technique for generating germline mosaics in *Drosophila melanogaster*. Genetics *144*, 1673–1679.
45. Tautz, D., and Pfeifle, C. (1989). A non-radioactive in situ hybridization method for the localization of specific RNAs in *Drosophila* embryos reveals translational control of the segmentation gene *hunchback*. Chromosoma *98*, 81–85.
46. Wieschaus, E., Nüsslein-Volhard, C., and Kluding, H. (1984). *Krüppel*, a gene whose activity is required early in the zygotic genome for normal embryonic segmentation. Dev. Biol. *104*, 172–186.
47. Gyuris, J., Golemis, E., Chertkov, H., and Brent, R. (1993). Cdi1, a human G1 and S phase protein phosphatase that associates with Cdk2. Cell *75*, 791–803.
48. Finley, R.L., Jr., and Brent, R. (1994). Interaction mating reveals binary and ternary connections between *Drosophila* cell cycle regulators. Proc. Natl. Acad. Sci. USA *91*, 12980–12984.
49. Gross, I., Georgel, P., Kappler, C., Reichhart, J.M., and Hoffmann, J.A. (1996). *Drosophila* immunity: A comparative analysis of the Rel proteins dorsal and Dif in the induction of the genes encoding Diptericin and Cecropin. Nucleic Acids Res. *24*, 1238–1245.
50. Clemens, J.C., Worby, C.A., Simonson-Leff, N., Muda, M., Maehama, T., Hemmings, B.A., and Dixon, J.E. (2000). Use of double-stranded RNA interference in *Drosophila* cell lines to dissect signal transduction pathways. Proc. Natl. Acad. Sci. USA *97*, 6499–6503.